

Compositional variations in strain-compensated InGaAsP/InAsP superlattices studied by scanning tunneling microscopy

B. Grandidier and R. M. Feenstra^(a)

Department of Physics, Carnegie Mellon University, Pittsburgh, PA 15213

C. Silfvenius and G. Landgren

Department of Electronics, Royal Institute of Technology, Kista, Sweden

Abstract

Cross sectional scanning tunneling microscopy (STM) and scanning tunneling spectroscopy are used to study strain compensated InGaAsP/InAsP superlattices grown by metalorganic vapor phase epitaxy, with or without an InP layer inserted in the InAsP barrier. A difference of contrast in the STM images is observed between the InAsP barrier grown over an InP layer compared with the InAsP barrier grown over the InGaAsP well. The first ≈ 4 nm of the InAsP barrier layers grown over the wells are found to be compositionally intermixed, containing significant enrichment of both arsenic and gallium atoms. This intermixing is believed to be due to some carry-over or surface segregation of these species when the growth is switched from well to barrier.

1 Introduction

The major approach for fabrication of semiconductor lasers operating at a wavelength of $1.3\mu\text{m}$ consists of the use of strained InGaAsP multiple quantum wells grown on InP substrates. For certain applications such as high-speed lasers and vertical cavity surface emitting lasers (VCSELs) a large number of wells is required. To enable the fabrication of a large number of strained wells, zero net-strain is achieved by counter-straining the barrier material. Wells with either compressive or tensile strain will both improve the laser performance due to separation of the light-hole and heavy-hole valence bands and a reduction of hole masses, resulting in a reduced density of states.[1] The dominating industrial fabrication method is metalorganic vapor phase epitaxy (MOVPE) and we have studied structures fabricated by this method. Structures utilizing tensile InGaP barriers have previously been studied by x-ray diffraction (XRD), photoluminescence (PL), scanning tunneling microscopy (STM) and device evaluation.[2,3] It was found that even though the material quality is excellent for structures with up to eight periods, the high bandgap of InGaP affects the hole transport in the MQW, resulting in an uneven carrier distribution in the active region, which reduces the device performance. Alternatively, for structures with tensile wells, compressive InAsP barriers would allow both strain compensation and the possibility to optimize the barrier height to enable an even carrier distribution in the MQW. Such structures have previously been studied by XRD, PL and device evaluation.[2] The XRD and PL results indicated a reduced material quality compared to the structures with InGaP barriers but the device performance was considerably better in the InAsP-structures than for the InGaP-structures, indicating the importance of a good carrier distribution. To improve the understanding of the growth mechanisms of the InAsP barrier structures, we present in this paper cross sectional tunneling microscopy (STM) and spectroscopy studies of a series of InGaAsP/InAsP superlattices. with or without InP interlay-

ers in the InAsP barriers.

We report results from two structures: a 4 period superlattice with InGaAsP wells and InAsP barriers, and a 16 period superlattice which includes InP interlayers in the InAsP barriers. In the case of the 16 period superlattice, we observe undulations in the morphology of the $(1\bar{1}0)$ cross-sectional face, similar to those previously reported for InGaAsP/InGaAs structures.[3] However, in contrast to this prior work, we find for both the 4 period and 16 period structures that the InAsP barriers appear defective and intermixed when they are grown over the InGaAsP wells compared with those barriers grown over InP layers. Based on the observed contrast of the STM images, we argue that the barriers grown over the wells contain a quaternary layer extending ≈ 4 nm from the interface, with this layer containing both increased Ga content and increased As content compared to the targeted composition of the InAsP barrier.

2 Experimental Details

The samples were prepared by MOVPE at a pressure of 50 mbar, using trimethylindium (TMI), trimethylgallium (TMGa), AsH₃, and PH₃ as sources gases. The undoped structures were grown on sulfur-doped ($N_d = 5 \times 10^{18} \text{ cm}^{-3}$) InP substrates, at a substrate temperature of 680° C.[2] Two structures were studied: the first was a 16 period superlattice with layer compositions and thicknesses determined by x-ray diffraction (neglecting possible intermixing of the overgrown barriers) to be of 4.1 nm In_{0.39}Ga_{0.61}As_{0.93}P_{0.07} quantum wells and 4.0 nm InAs_{0.21}P_{0.79} + 10.0 nm InP + 4.0 nm InAs_{0.21}P_{0.79} barriers. The second structure was a 4 period superlattice consisting of a 7.0 nm In_{0.39}Ga_{0.61}As_{0.93}P_{0.07} quantum well and an 11.0 nm InAs_{0.21}P_{0.79} barrier. The individual layers thicknesses have an uncertainty of about ± 1 nm from the x-ray diffraction, but the overall period is accurate to ± 0.1 nm. The quantum wells and barriers have 1.2 % tensile and 0.7 % compressive lattice-mismatch strains respectively, relative to the InP substrate, so that the strain is nearly balanced. From the layer compositions and thicknesses, the bandgap in the barrier is calculated to be 1.11 eV and the effective bandgap in the well (corresponding to the energy difference between the first electron and hole subbands of the well) is 0.93 eV for the 7 nm well, and 0.95 eV for the 4.1 nm well.[2] Each structure was surrounded by a 240 nm InP buffer layer and a 150 nm InP cap. The gas switching sequences followed the general scheme of switching off the group-III flow(s) while maintaining the hydride flows, then changing to the new hydride flows and eventually starting the growth of the next material by switching on the new group-III flow(s). Interruption times of 0.5 s (to make the chamber empty of group III species) + 0.5 s (to saturate the chamber with the new group V flow) were employed throughout the growth of all samples in this study.

To perform cross-sectional STM measurements, the samples were cleaved to expose a $(1\bar{1}0)$ surface, in an ultra-high vacuum chamber with a base pressure $< 5 \times 10^{-11}$ Torr. Polycrystalline W tips were chemically etched and then cleaned by in-situ electron bombardment and characterized by in-situ field emission microscopy. Images were obtained with a constant tunnel current of 0.1 nA, and sample voltages as described below. Growth direction is from the right to the left in all images. Details of the STM design [4], cleavage procedure [5], and spectroscopic methods [6] have been described elsewhere.

3 Results and Discussion

Figures 1(a) and (b) show large scale STM images of the 16 period InGaAsP/InAsP superlattices

containing an InP interlayer inserted in each InAsP barrier layer. These empty and filled states images were acquired at two different locations on the same sample. Several features are worth noting. First, a large surface undulation is observed, as shown by the cross-sectional cuts. For the part of the superlattice close to the cap layer, this undulation has a periodicity of 220 ± 20 nm in the [110] direction and its amplitude is about 6.5 \AA . The undulation has also been observed for other heterostructures [3,7] and arises from the relaxation of strain accumulated in the superlattice during the growth. Second, the interfaces between superlattice layers are relatively rough, as seen most clearly in Fig. 1(a) and examined in more detail below. Third, it is important to note that the right-most superlattice layer appears white (*i.e.* higher tip height) in both Fig. 1(a) and (b). This layer is an InAs_{0.21}P_{0.79} barrier, and we consistently observe white contrast for this barrier layer independent of the sample-tip voltage. Finally we note in Fig. 1 the presence of small white specks in the image (seen most clearly in Fig. 1(a)), appearing as some sort of “contamination” on the surface. These features actually arise after extended STM imaging at negative sample voltage, and we believe them to be associated with some unintentional transfer of material between the tip and sample.

Figure 2 is a high resolution image of a single period from the 16 period superlattice. For both signs of the sample voltage, it confirms the brightness of the first grown InAsP barrier in comparison with the well and the second barrier. To explain the difference of contrast between the various layers seen in the STM images, both the electronic variation along the superlattice due to the confinement of electrons and holes in the well, and the true topographic variation must be taken into account. Indeed, the relaxation of the strain during cleaving, which causes the large surface undulation already mentioned above, can also affect the topography of the surface at a smaller scale: the compressive layers tend to rise out of the $(1\bar{1}0)$ face whereas the tensile layers tend to be lowered.[7] The electronic and mechanical (elastic strain relaxation) contrast mechanisms are illustrated in Fig. 3 for the case of a compressive barrier and tensile well. Since the InAsP barriers in Fig. 2 appear *brighter* (higher tip height) than the quantum wells, we conclude that the relaxation of the strain is the dominant factor to explain the tip height variation on the superlattice. Another important feature to note in Fig. 2 is that the second barrier layer, *i.e.* the one grown on top of the InGaAsP well, is not clearly seen in the image. This layer has contrast similar to that of the well, so that the interface between this barrier and the well is difficult to localize. Thus, InAsP barrier layers grown on top of the quantum wells do not appear to have the expected chemical composition.

Figure 4 shows the 4 period superlattice, with the InP buffer layer on the right-hand side of the image. This superlattice does not contain any InP interlayers. The barriers again appear brighter than the wells for the reason already mentioned above. The intended position between the different layers is indicated by black lines at the top of the image. As found for the 16 period superlattice in Fig. 2, the interface between the well and the overgrown barrier is not at the intended position. Aside from the first barrier, the other barriers look thinner and the wells seem to extend into the barrier layers. Thus, the right-hand side of the intended barrier layers appear dark (similar to the wells) and the left-hand side of the barrier is bright, implying some sort of intermixing between the quantum wells and the overgrown barrier layers.

Another feature worth noting in Fig. 4 are the faint fringes aligned along the [110] direction seen in the quantum well layers. These fringes have a period of 23 \AA , corresponding to 4 unit cells

in the [001] direction. We have previously reported the observation of such “fourfold” periodicity, and we tentatively associated it with atomic ordering in the alloys. [3] However, we now know this explanation in terms of atomic ordering is incorrect, since, with exceptional probe tips, we have observed the fourfold periodicity at locations around point defects and step edges in the InP substrate (*i.e.* not on an alloy layer). [8] The fourfold periodicity is induced near defects, including the interfaces in the superlattice structures, in much the same way that the surface-state related electron standing waves are seen on metal surfaces.[9] However, observation of this feature on the InP and related alloy semiconductor layers is highly dependent on the tip condition. Possible explanations for this fourfold periodic feature will be discussed elsewhere.

In Fig. 5(a), we present a high resolution view of the 4 period superlattice along with its associated conductance image, Fig. 5(b). The contrast in Fig. 5(a) is quite different than that of Fig. 4 due to the different sample voltage and tip conditions. However, Fig. 5(b) clearly displays the periodicity of the superlattice. We position the InGaAsP quantum well and InAsP barrier layers as shown in the lower portion of the figure for two reasons: First, the contrast seen in the conductance image (smaller conductance over the quantum well) is consistent with that expected for conductance images acquired at constant current.[10] Second, spectroscopic measurements on the barrier layers marked in Fig. 5 do indeed reveal the expected bandgap for the barrier, as shown below. We also note in Fig. 5(a) the presence of the bright white lines, marked by the arrows at the top of the image. These bright atomic rows, having the periodicity of the superlattice, are also seen in Fig. 6 below and have been reproducibly observed in many of the STM images. We surmise that these rows are necessarily associated with an interface between quantum well and barrier, since no other discontinuities in growth exist elsewhere in the structure.

Figure 6 displays again two periods of the 4 period superlattice at high resolution. The positions of the wells and the barriers have been obtained by comparing this figure with Fig. 5(a), with the bright atomic rows (separating barrier and overgrown well) marked by arrows at the top of the image. The superlattice period obtained by counting the atomic rows in Fig. 6 is 17.6 ± 0.3 nm, in agreement with the XRD value of 18.0 ± 0.1 nm. In terms of the contrast of the various layers, we find that the left side of the InAsP barrier layers is bright, and the right side is dark. Although the contrast between the layers in Fig. 6 is less pronounced than that in Fig. 4, the width of these bright regions correspond closely to the widths of the bright barrier regions seen in Fig. 4. We interpret the bright portion of the barrier layers as being the intended (*i.e. not* intermixed with the well) portions of the barrier layer. These bright portions of the InAsP barriers were not observed in the 16 period superlattice for the barriers overgrown on the wells because the barrier thickness in the 16 period superlattice are only about one third of the barrier thickness in the 4 period superlattice. Alternatively, the dark part of the InAsP barrier layers is visible in both superlattices.

To characterize more fully the electronic properties of the superlattice we have performed measurements of spatially resolved spectroscopy. The spatial resolution in this case was somewhat crude, obtained simply by positioning the probe tip over apparent bright and dark regions in the topographic images as shown by the markers R1 and R2 at typical locations in Fig. 6. From our deduced position of the barrier and well, it is clear that the position of R2 is in the bright part of the barrier region. However, the precise position of R1 is not so clear, since it is located near the interface between well and overgrown barrier layers. The spectra of the normalized conductance versus sample bias are plotted in Fig. 7. Both spectra display well defined band edges, as marked by

dashed lines in Fig. 7. The nonzero conductance observed within the gap is the “dopant induced” component, which arises from tunneling out of filled conduction band states.[11] The measured bandgap of region R2 is 1.30 ± 0.10 eV is close to the calculated bandgap 1.11 eV of the InAsP barrier. The measured bandgap of region R1, 1.05 ± 0.10 eV, is similarly close to the calculated effective bandgap 0.93 eV of the InGaAsP well, indicating that this spectrum was either acquired over the quantum well region or that the dark regions of the barrier layers (near to the interface of barrier on well) have this value of relatively small band gap.

Let us now consider an interpretation of the above results in terms of the composition of the barrier and well regions. It is clear from our results that the barrier layers grown on top of the wells undergo some significant compositional intermixing in the first ≈ 4 nm of their thickness. For the 16 period superlattice, which has targeted thickness of the barrier layers of only 4 nm, this intermixing results in the complete absence of the barrier layers in the STM topographic images (*e.g.* Fig. 2). Alternatively, for the 4 period superlattice with targeted barrier layers thickness of 11 nm, some part of the “non-intermixed” barrier survives in the images (*i.e.* the bright part of the barriers in Figs. 3–5), although this region is thinner than the targeted thickness. Thus, we conclude that when the growth is switched from the well to the barrier materials, the first portion of the barrier grows with some unintended composition. This type of phenomenon has been previously observed, and attributed to arsenic carry-over during the MOVPE growth process or to a thermal As/P interdiffusion process.[12] For the group III species, surface segregation is found to be significant during growth of alloy layers.[13] In our case, we feel that an arsenic related process alone would not produce the observed contrast in the STM images, since arsenic would produce both a *smaller* band gap and a more *compressive* strain, both of which would lead to bright (*i.e.* higher tip height) contrast in the STM images in contradiction to our observation of *dark* contrast for the barrier on well regions.

To explain the observed images, it is necessary to invoke the presence of *gallium* in the portion of the barrier layers immediately on top of the quantum wells. This gallium could have its origin either in the carry-over in the growth reactor of gallium when switching from well to barrier growth,[14] or in some surface segregation of gallium atoms during growth of the wells (driven by the tendency of the quaternary quantum well to reduce its strain during growth) which would then supply gallium to the barrier layers. The observed dark contrast of the ≈ 4 nm of barrier layer on top of the wells could be accounted for by some combination of tensile strain in this intermixed layer as well as a possibly relatively large band gap. For example, referring to a diagram of bandgaps and strain for the InGaAsP system (see Fig. 1 of Ref. 2) if the intermixed layer contained about 30% Ga and 35% As, then it would have lattice constant similar to the quantum well but band gap similar to the barrier layer. Qualitatively, such a composition would be consistent with the observed STM images. Alternatively, slightly larger fractional compositions of 35% Ga and 45% As would give a similar lattice constant but a smaller band gap, which again could be consistent with the STM images. In either case, we see that making the transition from the $\text{In}_{0.39}\text{Ga}_{0.61}\text{As}_{0.93}\text{P}_{0.07}$ quantum wells to the $\text{InAs}_{0.21}\text{P}_{0.79}$ barriers produces this intermixed transition region with significant concentrations of both Ga and As.

4 Conclusion

We have performed cross-sectional studies STM imaging of InGaAsP/InAsP superlattices, grown by MOVPE with or without InP layers inserted in the InAsP barriers. These structures have re-

vealed a large scale elastic relaxation of the $(1\bar{1}0)$ cross-sectional plane as well as elastic relaxations of the different layers. This elastic relaxation of the layers is found to dominate in the observed contrast of the STM topographic images. The first ≈ 4 nm of the barrier layers grown over the wells are compositionally intermixed, and appear in the STM topographic images as more similar to the well material than the rest of the barrier layer. In conductance images, however, the thickness of the barrier and well layers are relatively close to those values targeted in the growth. We conclude that there is significant enrichment of both arsenic and gallium in this first portion of the barrier layers, caused by some type of carry-over or surface segregation of these species when the growth is switched from well to barrier.

We thank Huajie Chen for assistance with the finite element computations referred to in Fig. 3. This work was supported by a grant from the National Science Foundation, DMR-9615647

(*a*)Electronic mail: feenstra@andrew.cmu.edu

- [1] L. A. Coldren and S. W. Corzine, *Diode Lasers and Photonic Integrated Circuits* (Wiley-Interscience), p. 161, 502-507.
- [2] C. Silfvenius, B. Stålnacke, and G. Landgren, *J. Cryst. Growth* **170**, 122 (1997).
- [3] R. S. Goldman, R. M. Feenstra, C. Silfvenius, B. Stålnacke, and G. Landgren, *J. Vac. Sci. Technol. B* **15**, 1027 (1997).
- [4] R. M. Feenstra, 21st Int. Conf. Phys. Semicond., ed. P. Jiang and H.-Z. Zheng (World Scientific, Singapore, 1992), p.357.
- [5] R. M. Feenstra, E. T. Yu, J. M. Woodall, P. D. Kirchner, C. L. Lin, and G. D. Pettit, *J. Vac. Sci. Technol. B* **61**, 795 (1992).
- [6] P. Mårtensson and R. M. Feenstra, *Phys. Rev. B* **39**, 7744 (1988).
- [7] H. Chen, R. M. Feenstra, R. S. Goldman, C. Silfvenius and G. Landgren, *Appl. Phys. Lett.* **72**, 1727 (1998).
- [8] H. Chen, B. Grandidier, R. M. Feenstra, to be published.
- [9] M. F. Crommie, C. P. Lutz, D. M. Eigler, *Nature* **363**, 524 (1993); Ph. Hofmann, B. G. Briner, M. Doering, H.-P. Rust, E. W. Plummer, A. M. Bradshaw, *Phys. Rev. Lett.* **79**, 265 (1997).
- [10] J. A. Stroscio, R. M. Feenstra, D. M. Newns, A. P. Fein, *J. Vac. Sci. Technol. A* **6**, 499 (1988).
- [11] R. M. Feenstra, *Phys. Rev. B* **50**, 4561 (1994).
- [12] A. Mircea, A. Ougazzaden, J. Barrau, J.-C. Bouley, B. Calva, J. Charil, C. Kazmierski, G. Leroix, Proc. Conf. on InP and related Materials, Paris 1993; A. R. Clawson, X. S. Jiang, P. K. L. Yu, *J. Cryst. Growth* **147**, 8 (1995).
- [13] O. Brandt, L. Tapfer, K. Ploog, R. Bierwolf, and M. Hohnstein, *Appl. Phys. Lett.* **61**, 2814 (1992).
- [14] B. P. Keller, H. G. Bruhl, W. Seifert, *Crystal Research and Technology*, **27**, 617 (1992).

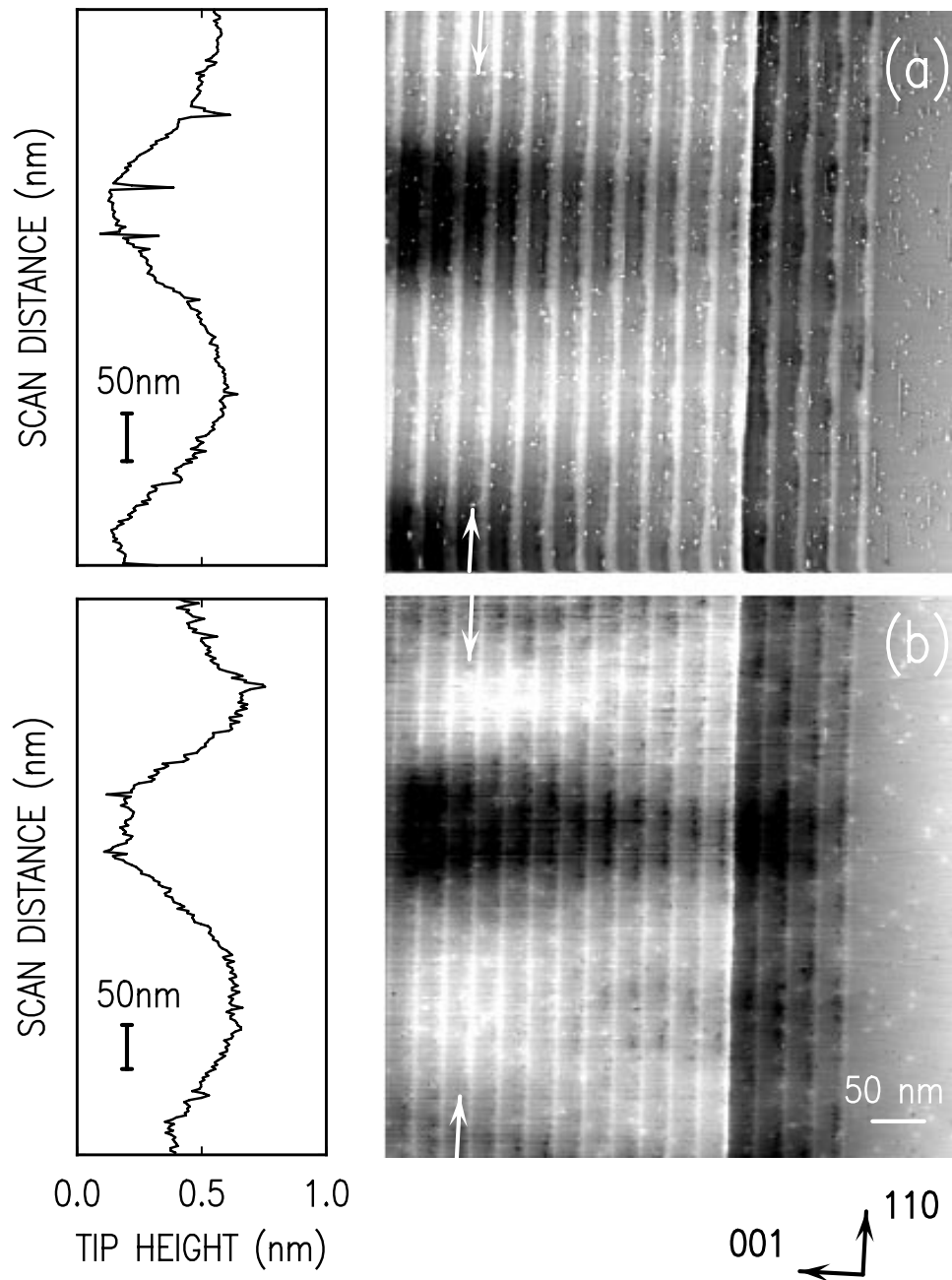


Figure 1 Large-scale topographic images of a 16 period InGaAsP/InAsP/InP superlattice acquired at sample voltages of (a) -2.0 V and (b) +2.3 V. Line cuts through the STM images in the [110] direction are displayed at the position indicated by arrows. Tip height is indicated by a grey scale, ranging from 0 (black) to 7 Å (white). On both images, a step occurs at the beginning of the 5th period. In these and all other images below, the growth direction is from right to left.

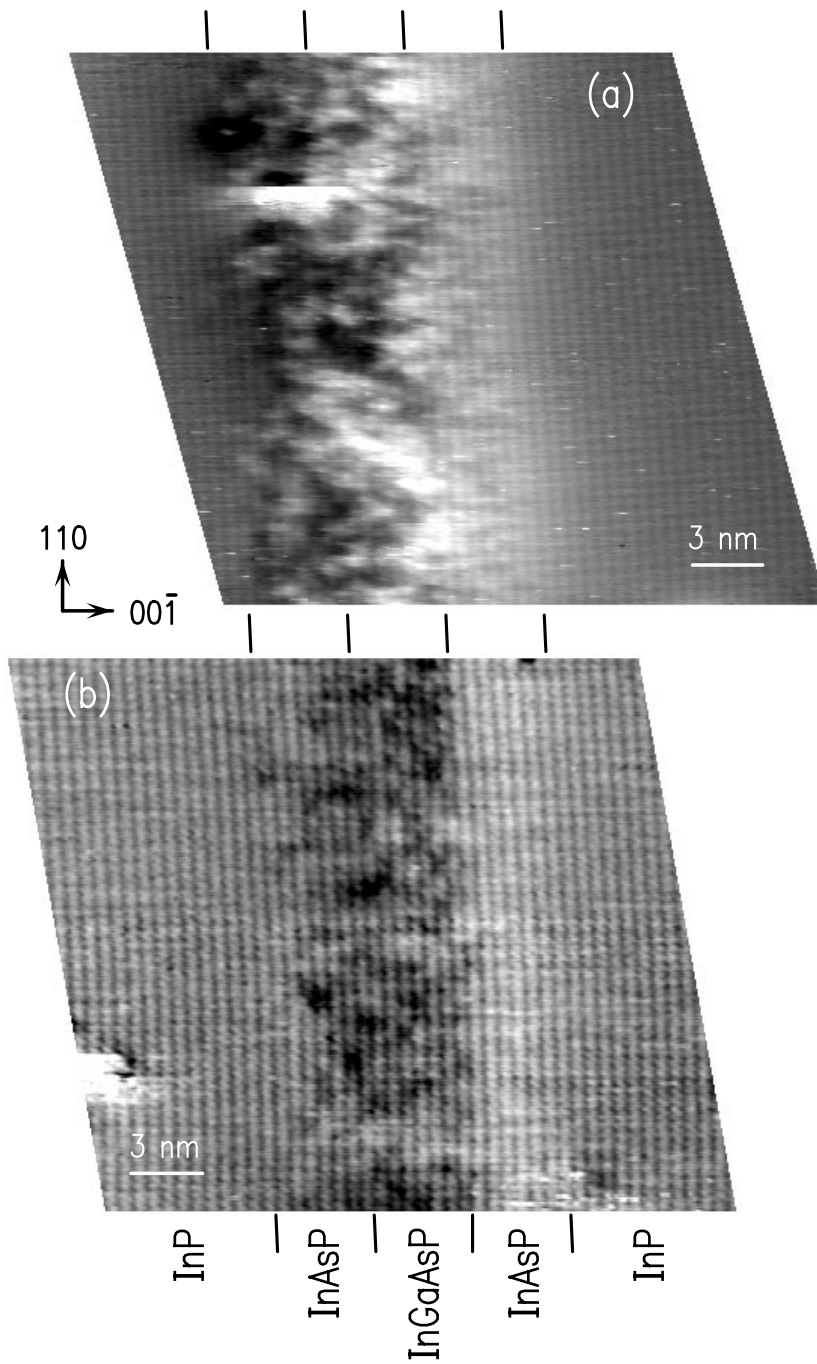
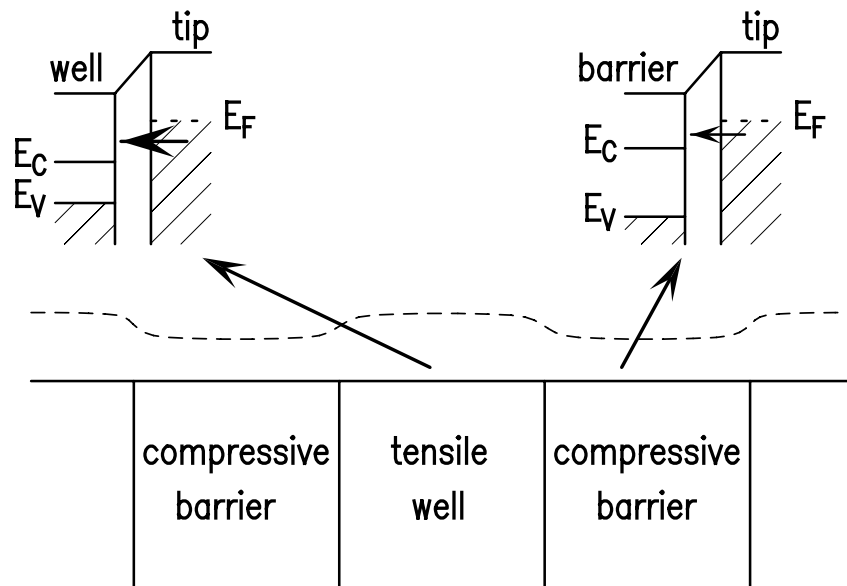


Figure 2 Close up views of a single period of the InGaAsP/InAsP/InP superlattice. Image (a) was acquired at a sample voltage of -2.3 V and image (b) at a sample voltage of +2.3 V. The intended position of the interfaces between the InP, InAsP, InGaAsP layers are indicated by the black lines extending in the [110] direction outside the images. The grey-scale ranges are (a) 2.4 Å and (b) 2.0 Å.

(a) Electronic



(b) Mechanical

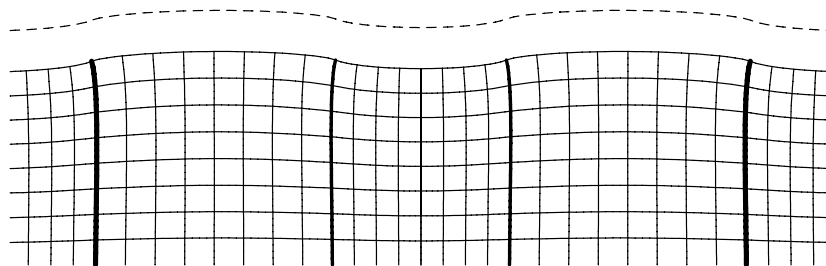


Figure 3 Illustration of STM contrast mechanisms for a strained semiconductor superlattice containing quantum wells in tension and barrier layers in compression. The dashed line shows the constant-current contour followed by the STM probe tip considering (a) only electronic, and (b) only mechanical effects. For case (a), the barrier has a larger band gap than the quantum well, so for a given tip-sample voltage there are fewer states available for tunneling to the barrier. Thus, a lower current is produced for a fixed tip-sample separation, so that the tip moves towards the sample to maintain a constant tunnel current. For case (b), relaxation of the strain produces an undulating surface morphology across the superlattice. For a strain of $\pm\epsilon$ in the layers and width of both barrier and well of L , the peak-to-peak amplitude $2h$ of the undulations is computed by finite elements to be $h / \epsilon L \approx 1.0$ for Poisson ratio of 0.35.

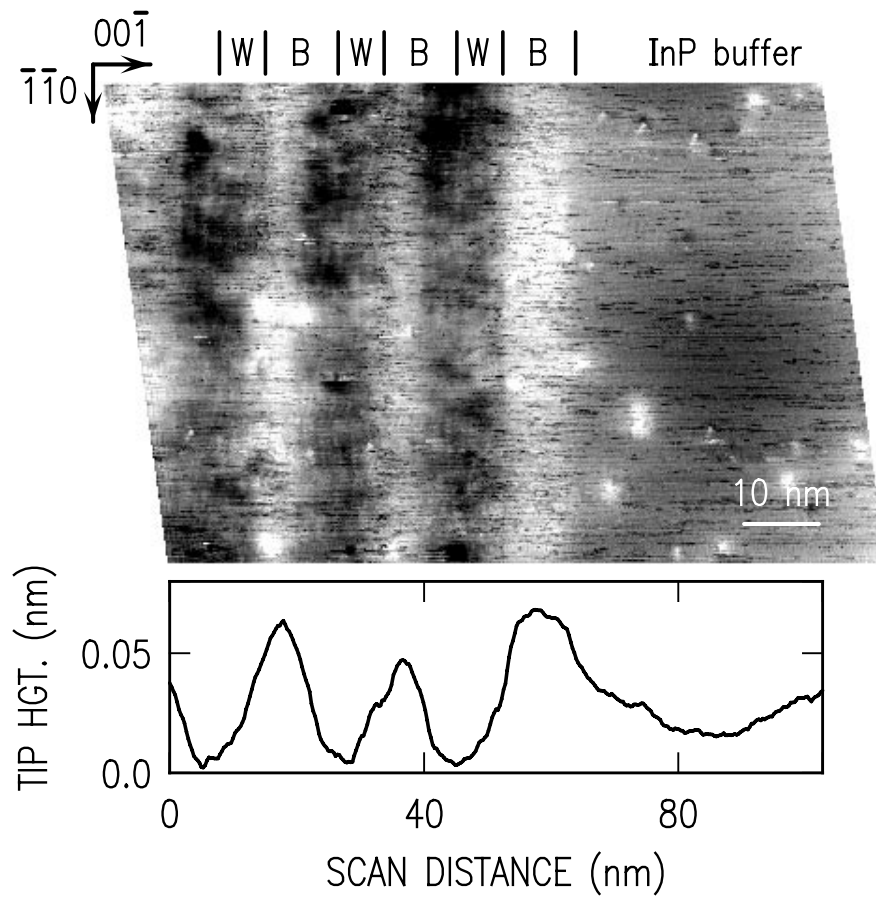


Figure 4 Topographic images of the 4 period InGaAsP/InAsP superlattice acquired at a sample voltage of +2.0 V. Fringes extending in the $[110]$ direction are faintly observed in the quantum wells. The intended position of the interfaces between the barrier (B) layers and the wells (W) layers is indicated by lines extending in the $[110]$ direction (see text). The grey-scale range is 1.7 \AA .

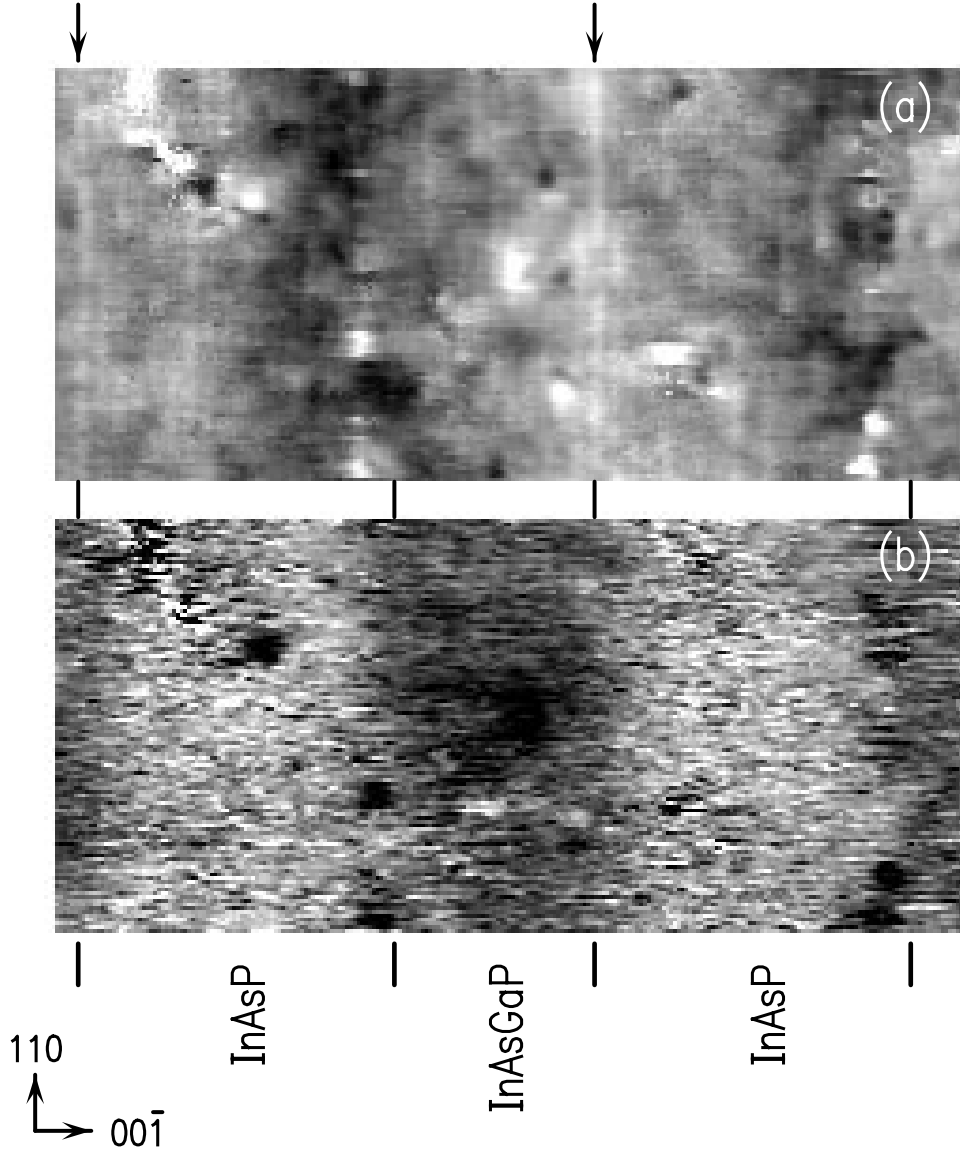


Figure 5 High resolution images of the 4 period InGaAsP/InAsP superlattice in image (a). Image (b) is a conductance image. Both images were acquired at the same sample voltage of -2.2 V. The intended position of the interfaces between the InAsP layers and the InGaAsP layers is indicated by lines extending in the $[110]$ direction. The brightest row in each period, located at the interface between a barrier and an overgrown well is indicated by an arrow. The grey-scale range is 1.3 Å.

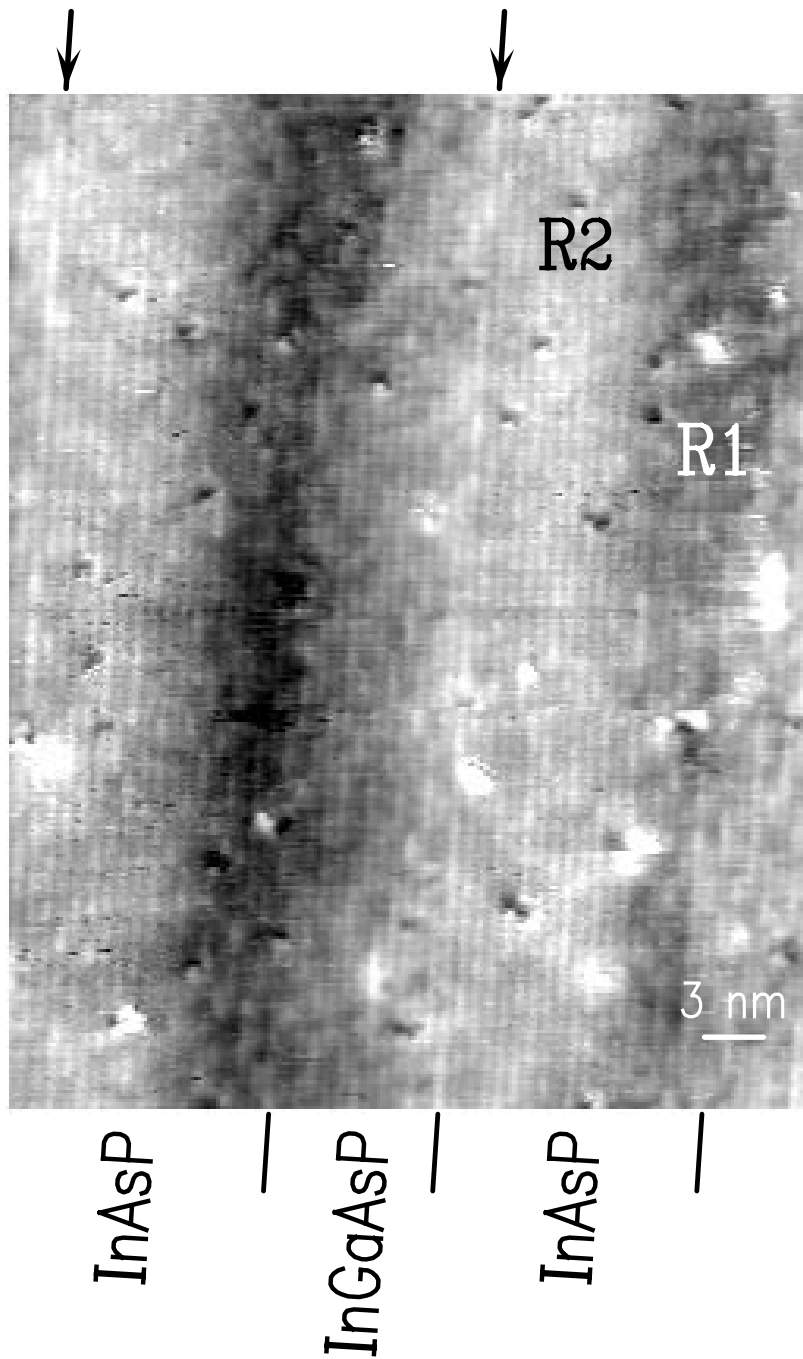


Figure 6 High resolution image of the 4 periods InGaAsP/InAsP superlattice, acquired at a sample voltage of -2.2 V. The brightest row in each period is indicated by an arrow. Regions R1 and R2 are two regions with an opposite contrast in an InAsP barrier. The grey-scale range is 1.3 Å.

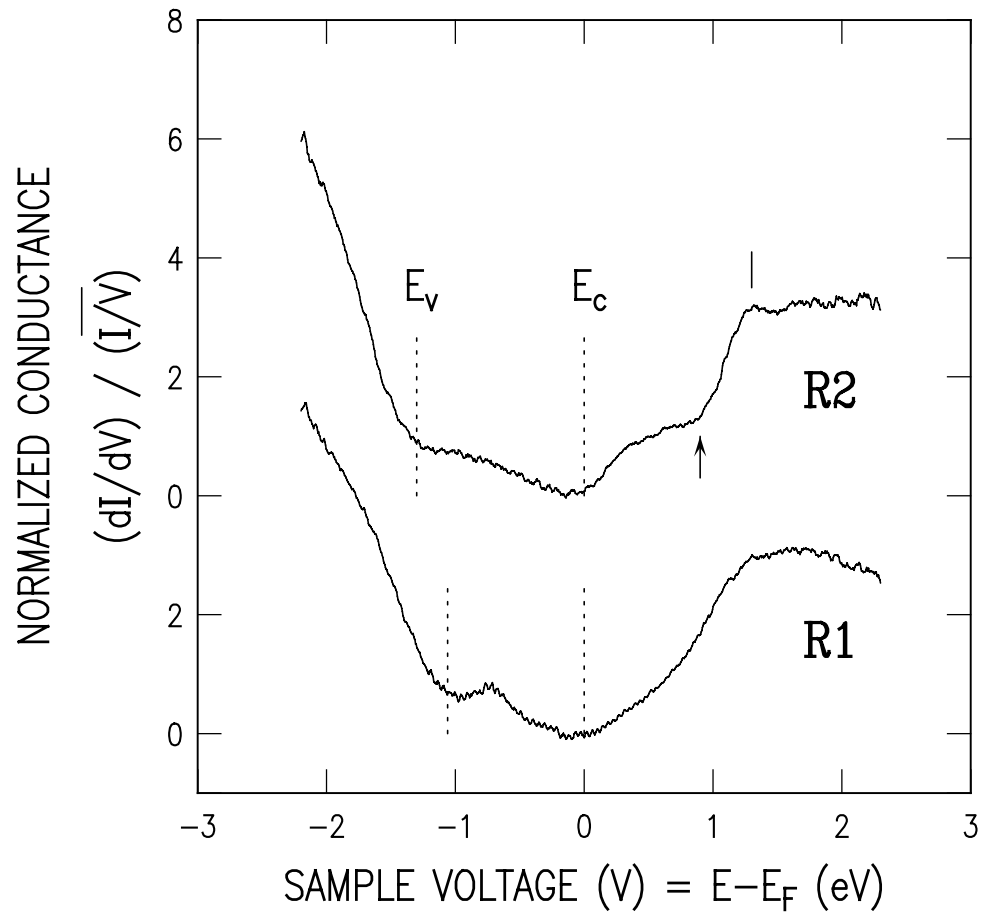


Figure 7 Spatially resolved spectroscopy results, acquired in regions R1 and R2 of the InAsP barriers. The valence band and the Γ valley conduction band edges are indicated by dotted lines, labeled E_v and E_c respectively. Onset of the L-valley conduction band is indicated by an upward pointing arrow. A surface state peak is marked by a thin vertical line.